Supporting Information

Bifacial Four-Terminal Perovskite/Silicon Tandem Solar Cells and Modules

G. Coletti[1,2], S.L. Luxembourg[1], L.J. Geerligs[1], V. Rosca[1], A.R. Burgers[1], Y. Wu[1], L. Okel[1], M. Kloos[1], F.J.K. Danzl[1], M. Najafi[3], D. Zhang[3], I. Dogan[3], V. Zardetto[3], F. Di Giacomo[4], J. Kroon[1], T. Aernouts[5], J. Hüpkes[6], C.H. Burgess[7], M. Creatore[7], R. Andriessen[3], S. Veenstra[3]*

[1] TNO Energy Transition, Solar Energy, Westerduingweg 3, 1755LE, Petten, the Netherlands

[2] School of Photovoltaic and Renewable Energy Engineering, UNSW, Sydney, New South Wales 2052, Australia

[3] TNO Energy Transition, partner in Solliance, High Tech Campus 21, 5656 AE Eindhoven, the Netherlands

[4] Now at: Centre for Hybrid and Organic Solar Energy, Department of Electronic Engineering, University of Rome Tor Vergata, Via del Politecnico 1, 00133, Rome, Italy

[5] IMEC, partner in Solliance, Thin Film PV, Thor Park 8320, 3600 Genk, Belgium

[6] IEK5-Photovoltaics, Forschungszentrum Jülich, 52425 Jülich, Germany

[7] Department of Applied Physics, Eindhoven University of Technology, P.O. Box 513, 5600 MB Eindhoven, The Netherlands

Corresponding Author

*E-mail: gianluca.coletti@tno.nl

Supporting Information

Why bifacial?

Recently, bifacial PV silicon module technology has been rapidly gaining market share[1] because of their increased energy yield over conventional monofacial modules, which comes at almost no extra cost compared to a monofacial bottom device. In addition, because of the replacement of the traditional backsheet with glass, manufacturers can extend the power output warranty to 30 years instead of the present 25 years. Bifacial modules are capable of collecting light falling onto their front and rear surfaces, thereby increasing carrier generation.

Comparison 2T versus 4T bifacial Tandem

In a 4-terminal configuration the extra power generated by the bifacial bottom device scales linearly with the rear irradiance . In a 2-terminal configuration the power production is limited by the requirement for current matching of top and bottom cells. Therefore, the bifacial 2-terminal tandem device needs to be designed such that the top device absorbs more photons in order to match the extra current generated in the bifacial bottom device. This can be done by incorporating a thicker perovskite absorber layer or by lowering the band gap of the top perovskite cell and/or by other technological approaches[2]. While current gain by increased thickness is limited, lowering of the bandgap reduces the voltage gain advantage of the tandem concept. Importantly, appropriate tuning of the 2T configuration requires simulation of real outdoor conditions in order to maximize energy output[2, 3, 4]. Recently, it was shown that for a number of geographical locations and using common soil types (sand or grass) a current mismatch of 6 mA/cm^2 under STC conditions (monofacial) would be optimum.[5] A comparison of the annual energy yield of bifacial 2T and 4T tandems will be made in a forthcoming publication. Although this customization might be challenging in a production environment, we still think that a bifacial proposition for 2T tandem can still be beneficial in term of extra energy yield when the right technology adaptation are taken care of[2].

Energy yield input parameters

Key factors in the decision whether or not a PV plant will be realized on a certain location involve the investment costs and energy yield. In general, the energy yield will depend not only on the STC efficiency of the module but also on the design parameters of a PV plant (location, orientation, row spacing etc.). In the particular case of bifacial modules the actual bifacial gain will depend on these parameters, as well as on the albedo of the surroundings, the height of the installation, etc. At TNO Energy Transition, we have developed and extensively validated the modeling software BigEye[6] to calculate the annual energy yield of bifacial systems. On the basis of location-specific irradiance (global horizontal and diffuse horizontal irradiance) and meteorological data (temperature and wind speed) the annual power output of PV systems of widely varying geometrical designs can be calculated.

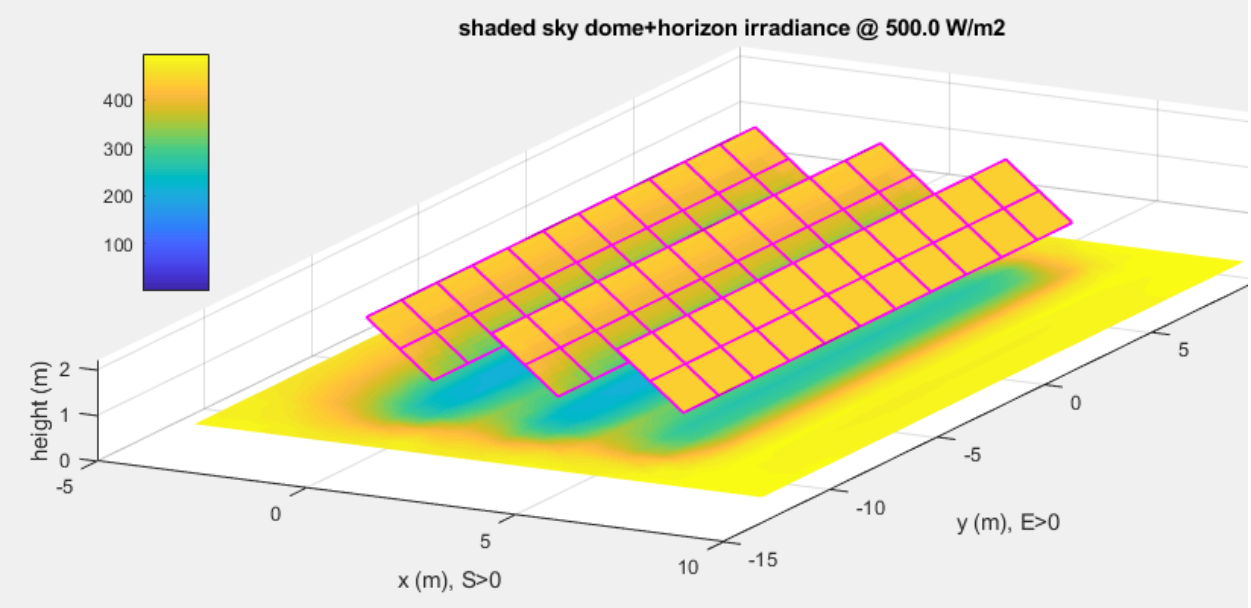

Figure SI 1. BigEye PV system configuration. Shed, South facing, 3 rows of 11x2 modules (1.65m² each, not in scale in the figure).

The results described in the main text of the paper were obtained for a south facing shed configuration with three rows of 22 modules each in landscape orientation with two modules height. Each module area is 1.65 m^2. Two strings per row (string of top and string of bottom modules), with 3 bypass diodes per module. The ground clearance is 1m and afixed tilt angle of 37° for Amsterdam and 40° for Denver were applied. Figure S1 includes a schematic representation of the system analysed in BigEye. The albedo of the surroundings was set at 30%. The ground coverage ratio (GCR) which is defined as the ratio of the array length (vertical) to the row-to-row distance (pitch) is varied by varying the pitch between 3 and 9 meters. The spectral composition of the front and rear irradiance were not taken into account. Only the power output of the center row of three rows of modules was simulated, eliminating edge effects on irradiance that would overrate bifacial systems.

The equivalent efficiency is defined as the efficiency of a hypothetical monofacial device that would generate the same amount of energy output as the real bifacial device, under the same operating and location conditions. We define this as the 'energy equivalent efficiency' or simply 'equivalent efficiency' of a monofacial device:

$$\eta_{equivalent} = \eta_{mono,ref} \times \left(1 + \frac{E_{Tandem,bifi} - E_{mono,ref}}{E_{mono,ref}}\right) \quad (1)$$

where $\eta_{equivalent}$ is the energy equivalent efficiency, $\eta_{mono,ref}$ is the efficiency of the reference monofacial module, $E_{Tandem,bifi}$ is the annual energy yield of the bifiacial tandem module and $E_{mono,ref}$ is the annual energy yield of the monofacial reference module.

The outcome of the simulation for Amsterdam is included in the main text. In Figure S2 the results of the simulation for Denver, Colorado are shown (for details see main text).

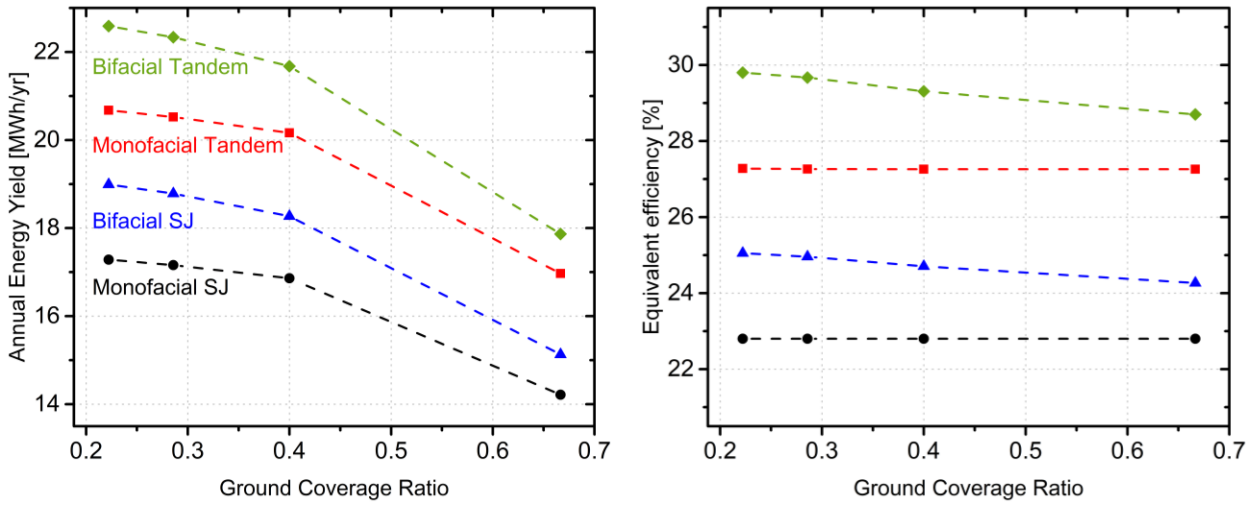

Figure SI 2. Left: Comparison of the modeled annual energy yield from the central row (22 modules 1.65 m²) for tandem PV plants as described in the text, obtained from the BigEye analysis using Denver, CO, United States of America as location, and a ground surface albedo of 30%. Right: When normalized on the monofacial c-Si MWT-SHJ annual energy yield, an equivalent efficiency is determined, which for the bifacial systems varies significantly with the GCR, and for the bifacial tandem approach 30%.

4 Terminal measurements

The perovskite solar cell is measured with a NeonSee sun simulator class AAA. The MWT-SHJ cell is measured with a Wacom class AAA solar simulator[7,8]. Since the perovskite and the c-Si bottom cells used in this study have very different areas, they cannot be measured simultaneously in a tandem configuration[9]. Therefore, their 4T performance was derived from the IV characteristics of the ST-PSC and the filtered bottom cell (Table S1) by adding the top and bottom cell contributions.

$$\eta_{Tandem} = \eta_{top} + \eta_{bottom} \tag{2}$$

The efficiency of the bottom device is:

$$\eta_{bottom} = \frac{V_{oc} FF J_{sc,bottom}}{100\ mW/cm^2} \tag{3}$$

The EQE of the bottom device is determined by multiplying the measured EQE of the single junction device with the measured transmittance of the perovskite solar cells (see Figure SI 3). The short circuit current of the bottom device ($J_{sc,bottom}$; Eq. 4 filtered bottom cell as reported in Table SI 1) is determined by multiplying the J_{sc} single junction (from IV measurement; Table I) by the ratio of the J_{sc} determined from the calculated EQE of the bottom device and the J_{sc} determined from the single junction EQE (Eq. 5 and see Figure SI 3). The Voc and FF were obtained from interpolation of IV measurements with a series of neutral density filters to arrive at the illumination level corresponding to $J_{sc,bottom}$.

$$J_{sc,bottom} = J_{sc,IV,single-junction} \frac{J_{sc,EQE,bottom}}{J_{sc,EQE,single-junction}} \tag{4}$$

$$J_{sc,EQE} = \int q \frac{\lambda}{hc} \mathrm{EQE}(\lambda) f(\lambda) Irr(\lambda)\, d\lambda \tag{5}$$

where EQE(λ) is the External Quantum Efficiency of the single-junction silicon cells, f(λ) = T(λ) for $J_{sc,EQE,bottom}$ with T(λ) being the transmittance of the top device and f(λ) = 1 for the $J_{sc,EQE,single\text{-}junction}$.

The difference in Voc and FF between this method and measuring the bottom device under the perovskite cells is negligible. Werner *et al*, compared bottom device IV measurements with either a neutral density filter or a long-wave pass filter obtaining overlapping IV characteristics[9,8].

We determined the 4T tandem output power for an additional rear irradiation of 10 mW/cm^2 or 20 mW/cm^2. In the new IEC measurement norm[10] for the characterisation of bifacial devices, peak power at these irradiance levels should be reported. To calculate the bifacial 4T performance, we add to $J_{sc,bottom}$ (Eq.4), the rear side contribution, according to:

$$J_{sc,bottom,BiFi} = J_{sc,bottom} + \frac{G_r}{100\ mW \times cm^{-2}} J_{sc,rear} \quad (6)$$

where $J_{sc,rear}$ is the short circuit current when the device is illuminated only on the rear side at STC (100 mW/cm^2) and G_r is the rear irradiance in mW/cm^2. Here, we take into account the V_{oc} gains and FF losses resulting from the additional current realized by the rear side illumination [11]. To do so, the V_{oc} and FF were obtained from interpolation of IV measurements with a series of neutral density filters to arrive at the illumination level corresponding to $J_{sc,bottom,BiFi}$. The η_{bottom} and η_{Tandem} follow from Eq. 3 and Eq. 2, respectively.

Table SI1. Overview of the I-V parameters of the semi-transparent PSC and c-Si bottom cells. The individual single-junction devices as well as the 4T tandem device is given at STC (viz. only front irradiance, 100mW/cm2, AM1.5g) and at two different levels of additional rear irradiance (10 mW/cm2, 20 mW/cm2 AM1.5g). Similarly, MWT-SHJ bifacial bottom cell efficiencies are reported as single junction devices and as bottom devices. Obviously these latter values include filtering by the perovskite top cell.

Device	Description	J_{sc} (mA /cm^2)	V_{oc} (mV)	FF (%)	Power density relative to front-incident irradiance of 100 mW/cm^2 (%)		
					Single-junction	Single-device for 4T tandem	4T tandem
ST-PSC Single-junction	Backward scan	21.0	1046	78.6	17.3		
	Forward scan	21.0	1041	78.0	17.0		
	Top cell – 5 min MPP tracking	-	-	-	17.0	17.0	
Bifacial MWT-SHJ Single-junction	Front illumination single junction (Bifi0)	39.4	730	79.4	22.8		
	Rear illumination single junction	34.1	728	76.9	19.1		
	Front illumination + rear 100W/m^2 (Bifi100)	42.8	733	79.2	24.8		
	Front illumination + rear 200W/m^2 (Bifi200)	46.2	735	79.0	26.8		
Bifacial 4T Tandem	Filtered bottom cell (Bifi0)	16.8	710	79.9		9.5	26.5
	Filtered bottom cell + rear 100W/m^2 (Bifi100)	20.2	715	79.9		11.5	28.5
	Filtered bottom cell + rear 200W/m^2 (Bifi200)	23.6	718	79.8		13.5	30.5

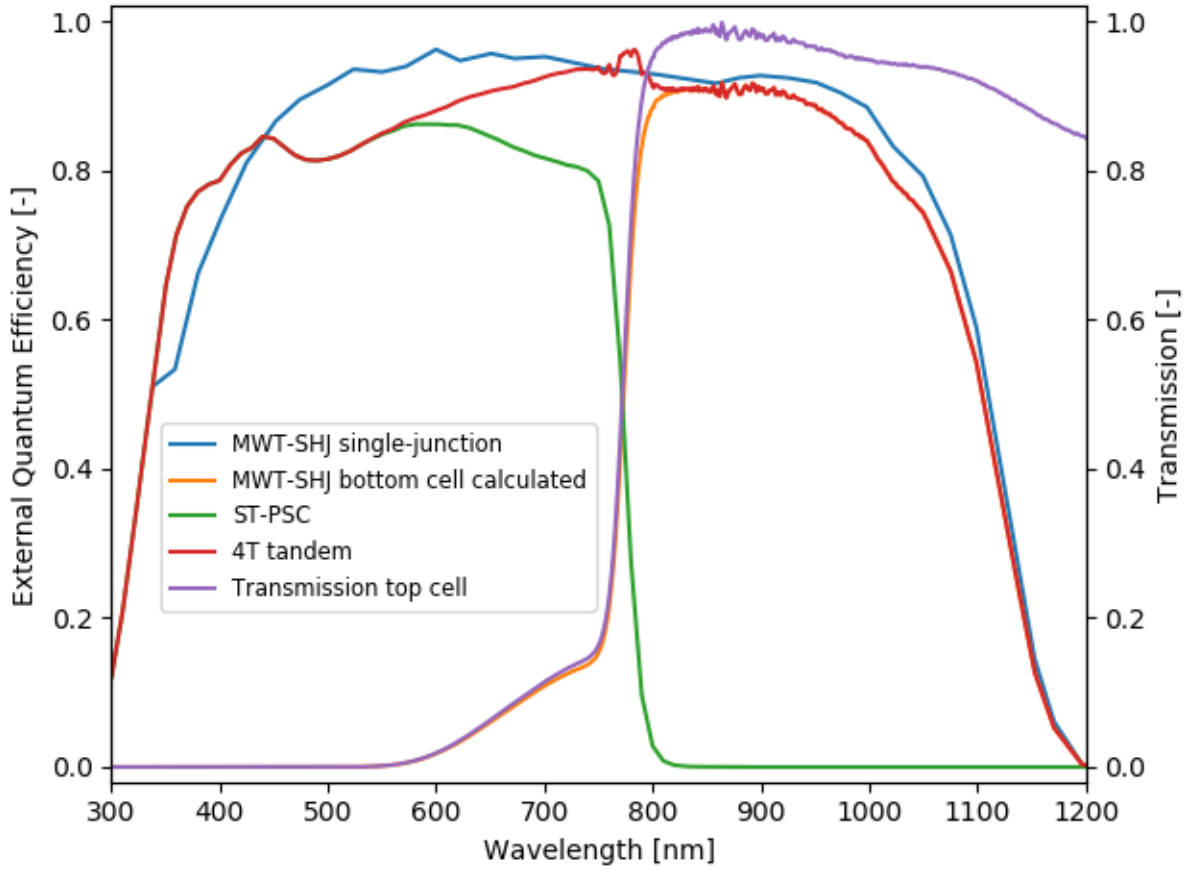

Figure SI 3. External Quantum Efficiency (EQE) of the single-junction MWT-SHJ (single-junction) cells, SemiTransparent perovskite solar cell (ST-PSC) and calculated bottom cell (MWT-SHJ bottom cell calculated). The total EQE of the 4-terminal Tandem device is also plotted. The transmission of the PSC is also plotted (secondary y axis).

Minimodule fabrication

The top and bottom devices were laminated in a three-chamber vacuum laminator (Phototrade, Italy) between two sheets of glass (D&K, The Netherlands) of 80x80x2.1 mm using an experimental thermoplastic material as encapsulant. The lamination cycle involved excursion to 140°C for ca. 5 minutes. The module stack was assembled under normal lab conditions (no special dry environment). The edge sealing – a combination of a silicone-based sealant and aluminum tape – provided protection against

moisture ingress for the duration of the outdoor monitoring.

Figure SI 4. Top: Configuration of the 4T tandem minimodules for outdoor testing. Bottom left: edge sealing scheme. Bottom right: 4T tandem minimodules for outdoor testing photo TNO Energy Transition, Solar Energy.

The monofacial module was coated with white paint on the air side of the rear glass sheet, to block the rear light and for better IR light management, which resembles commercial module configuration.

References (Supporting Information)

[1] International Technology Roadmap for Photvoltaic (ITRPV) – Results 2018, 10th ed; March 2019, itrpv.vdma.org.
[2] L.J. Geerligs, D. Zhang, G.J.M. Janssen, S.L. Luxembourg, 4-Terminal and 2-Terminal Tandem Modules in Bifacial Operation Model Analysis and Comparison, 35th European Photovoltaic Solar Energy Conference (2018) 676-680.
[3] R. Asadpour, R.V.K. Chavali, M.R. Khan and M.A. Alam, "Bifacial Si Heterojunction-Perovskite Organic-Inorganic Tandem to Produce Highly Efficient Solar Cell", Appl. Phys. Lett. 106 (2015) 243902
[4] S.L. Luxembourg, D. Zhang, M. Najafi, V. Zardetto, S. Veenstra, L.J. Geerligs, Perovskite/Crystalline Silicon Tandems: Impact of Perovskite Band Gap and Crystalline Silicon Cell Architecture, 33rd European Photovoltaic Solar Energy Conference (2017) 1176-1180.
[5] Dupré, Olivier, Rodolphe Vaillon, and Martin A. Green. "Physics of the temperature coefficients of solar cells." Solar energy materials and solar cells 140 (2015): 92-100.
[6] Janssen, G. J. M., A. R. Burgers, A. Binani, A. J. Carr, B. B. Van Aken, I. G. Romijn, Markus Klenk, Hartmut Nussbaumer, and Thomas Baumann. "How to maximize the KWH/KWP ratio: Simulations of single-axis tracking in bifacial systems." In International Conference EU PVSEC for Photovoltaics Research, 24-28 September 2018, Brussels, Belgium, 1-5. 2018.
[7] Coletti, G., Y. Wu, G. Janssen, J. Loffler, B. B. Van Aken, F. Li, Y. Shen et al. "20.3% MWT Silicon Heterojunction Solar Cell—A Novel Heterojunction Integrated Concept Embedding Low Ag Consumption and High Module Efficiency." IEEE Journal of Photovoltaics 5, no. 1 (2014): 55-60.
[8] Coletti, G., F. Ishimura, Y. Wu, E. E. Bende, G. J. M. Janssen, B. B. van Aken, K. Hashimoto, and Y. Watabe. "23% Efficiency metal wrap through silicon heterojunction solar cells." In 2016 IEEE 43rd Photovoltaic Specialists Conference (PVSC), pp. 2417-2420. IEEE, 2016.
[9] J. Werner, G. Dubuis, A. Walter, P. Löper, S.-J. Moon, S. Nicolay, M. Morales-Masis, S. De Wolf, B. Niesen, C. Ballif, C. Solar Energy Materials and Solar Cells 141 (2015) 407–413.
[10] IEC TS60904-1-2:2019 Photovoltaic devices - Part 1-2: Measurement of current-voltage characteristics of bifacial photovoltaic (PV) devices

[11] G.J.M. Janssen, B.B. van Aken, A.J. Carr, A.A. Mewe, Energy Procedia 77 (2015) 364 – 373 and Electric Power Research Institute EPRI, Bifacial Solar Photovoltaic Modules - Program on Technology Innovation (2016)